Optical Selection Rules in Light Emission from the Scanning Tunneling Microscope

M. Sakurai,[1,2] C. Thirstrup,[3] and M. Aono[1,2,4]

[1]*National Institute for Materials Science, Namiki, Tsukuba, Ibaraki 305-0044, Japan*
[2]*Nanoscale Quantum Conductor Array Project, ICORP, JST, Kawaguchi, Saitama 332-0012, Japan*
[3]*Vir A/S, Kuldyssen 10, 2630 Taastrup, Denmark*
[4]*Department of Material and Life Science, Osaka University, Suita, Osaka 565-0871, Japan*

(Received 7 March 2004; published 21 July 2004)

It is reported that optical selection rules still apply in light emission from the scanning tunneling microscope (STM). Linear polarization of isochromat light emitted from the tunneling gap between a STM tip made of tungsten (W) and a silicon (Si) sample with a (001) clean surface strongly depends on the bias voltage between tip and sample. The results show that π^* and σ^* surface states, for example, of the Si(001) sample contribute to emission of *p*- and *s*-polarized light, respectively, in accordance with optical selection rules.

DOI: 10.1103/PhysRevLett.93.046102 PACS numbers: 68.37.Ef, 73.20.–r, 74.25.Gz, 78.67.–n

Light emission from the tunneling gap between tip and sample of the scanning tunneling microscope (STM) was first reported by Gimzewski and co-workers [1] and, since then, a number of experimental and theoretical studies [2–6] have been performed on this notable phenomenon. For noble metal samples [2], the STM-induced light emission is considerably strong with a quantum efficiency of the order of 10^{-4} photons/electron, which is attributed to radiative decay of the tip-induced surface plasmon [3,4]. For semiconductor samples [5–7], different mechanisms dominate the STM-induced light emission, since the plasmon energy of semiconductors is in general far different from the photon energy of visible light, which is detected in usual experimental setups. For III-V semiconductors [5,6], electrons tunneling from a STM tip recombine with holes in the semiconductors resulting in strong luminescence with a quantum efficiency of the order of 10^{-4} photons/electron. Such a process, however, is forbidden for silicon (Si) due to its indirect band gap. Another mechanism of interest has been found for a Si sample in which no electron-hole recombination occurs [8]. Namely, it has been revealed that direct transitions between local surface states of the sample and local states of a STM tip occur, accompanied with light emission with an efficiency of the order of 10^{-6} photons/electron.

In the present work, we have found an experimental fact of great interest regarding the radiative direct transitions between tip and sample mentioned above. Namely, it has been found for a Si(001) sample that optical selection rules hold with respect to the orbital symmetries of relevant tip and sample states as the initial and final states of the direct transition. For example, transitions from a localized state of a STM tip made of tungsten (W) to the π^* and σ^* surface states of a Si sample with a (001) clean surface radiate *p*- and *s*-polarized light, respectively, in accordance with optical selection rules. Such experimental results not only give a direct proof of the occurrence of the radiative direct transitions between tip and sample, but also show that the orbital symmetries of surface states can be analyzed in an energy-resolved manner at the spatial resolution of the STM.

Experiments were carried out at room temperature using an ultrahigh vacuum STM (JEOL, JSTM 4000XV) with an electrochemically sharpened W tip. As shown in Fig. 1, two optical fiber bunches were placed near the tip-sample gap of the STM to collect light emitted from the gap in the following two different ways. The right fiber bunch collected linearly polarized light, whose polarization angle was determined by the transmission axis of a linear polarizer (Corning, Polarcor [9]) fixed at the front end of the fiber bunch with epoxy (see the inset of Fig. 1). By rotating the fiber bunch using a mechanical device, the axis of the polarizer can be rotated, so that *p*- and *s*-polarized light can be collected separately through the fiber bunch. On the other hand, the left optical fiber bunch was used to measure the total

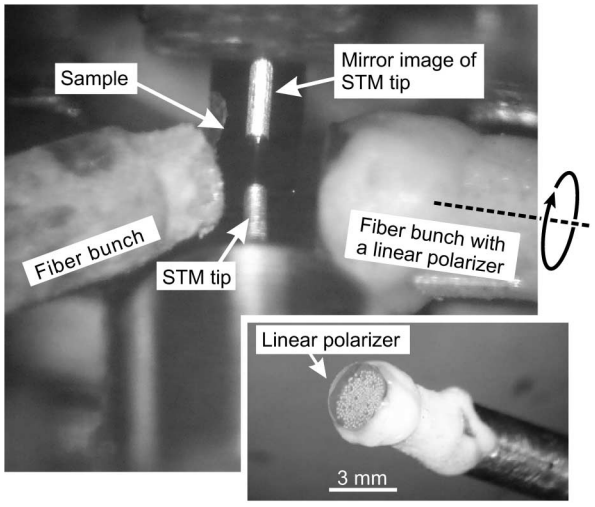

FIG. 1. The main part of the photon-detecting STM used in the present work. Two optical fiber bunches are placed close to the tunneling gap between tip and sample. The right fiber bunch has a linear polarizer at its front end. See the text for details.

intensity of emitted light as described in our previous papers [8]. In both cases, the collected light was guided to the outside of the chamber and its optical spectrum was measured by an optical system with a photomultiplier tube (Hamamatsu, R2949) and an optical band-pass filter.

A clean Si(001)-(2×1) surface (Sb doped, 1×10^{18} cm^{-3}) was used as a sample. The surface consists of regularly arranged Si dimers and each dimer has σ, π, σ^*, and π^* electronic states formed by Si $2p$ dangling bond orbitals [see Figs. 2(a) and 2(b)]. These electronic states are well separated in energy [10]. Actually, the Si dimers are buckled as shown in Fig. 2(c), but approximately the σ and σ^* states are formed by $2p_x$ orbitals and the π and π^* states by $2p_y$ and $2p_z$ orbitals as shown in Figs. 2(a) and 2(b), where the z axis is perpendicular to the surface and the x axis is parallel to the surface lying in the same plane as the dimer axis; the π and π^* states have a strong $2p_z$ character due to the buckling of the dimer [11,12].

When a W tip was positioned just above a Si dimer of a Si(001)-(2×1) surface, the intensity of emitted light at a fixed photon energy of $h\nu = 1.91$ eV (± 0.06 eV) was measured as a function of V_s at $I_t = 8$ nA by putting a band-pass filter in front of the optical detector, and the results are shown in Fig. 3(a). This intensity, measured by the left optical fiber bunch, is referred to as the total intensity I_{total} since it contains all components of polarization. The quantum efficiency of I_{total} was 0.4×10^{-6} photons/electron at the maximum intensity in Fig. 3(a). The light emission shown in Fig. 3(a) occurs by radiative direct electron transitions between tip and sample discussed in our previous paper [8] and is illustrated in Fig. 4 schematically; note that band bending due to the electric field produced by the STM tip [13] is taken into consideration in Fig. 4. Namely, the strong intensity around $V_s = -4.8$ V and the weak intensity around $V_s = -6.5$ eV in Fig. 3(a) are due to the radiative transitions from the π^* and σ^* states of the sample, respectively, to empty states of the tip, as shown in Figs. 4(a) and 4(b); the reason why the intensity around $V_s = -6.5$ eV is weak will be discussed later. Similarly, a peak at $V_s = +4.2$ V in Fig. 3(a) is due to the transitions from an

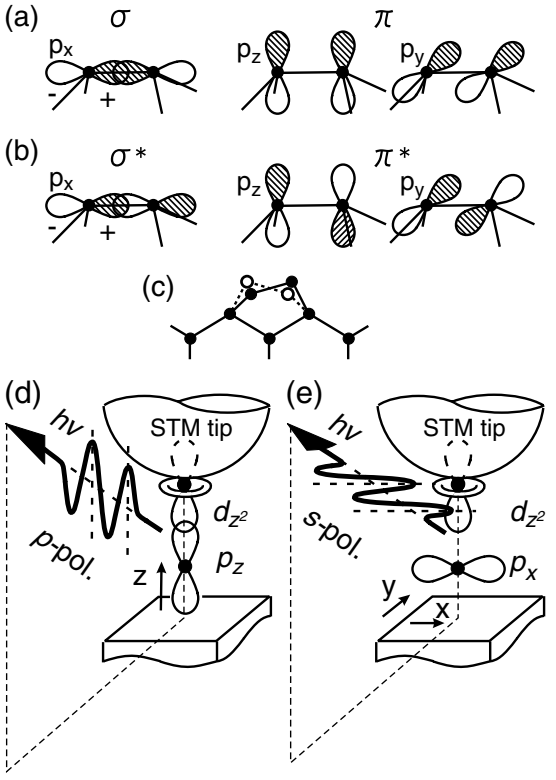

FIG. 2. Schematic drawing of Si $2p_x$, $2p_y$, and $2p_z$ orbitals that form (a) bonding and (b) antibonding states of a Si dimer on the Si(001)-(2×1) surface. As shown in (c), the Si dimer is actually buckled as illustrated with either open or filled circles, but a symmetric dimer is assumed in (a) and (b) for simplicity. Schematic illustration of (d) p- and (e) s-polarized light creation by the radiative transition between tip and sample.

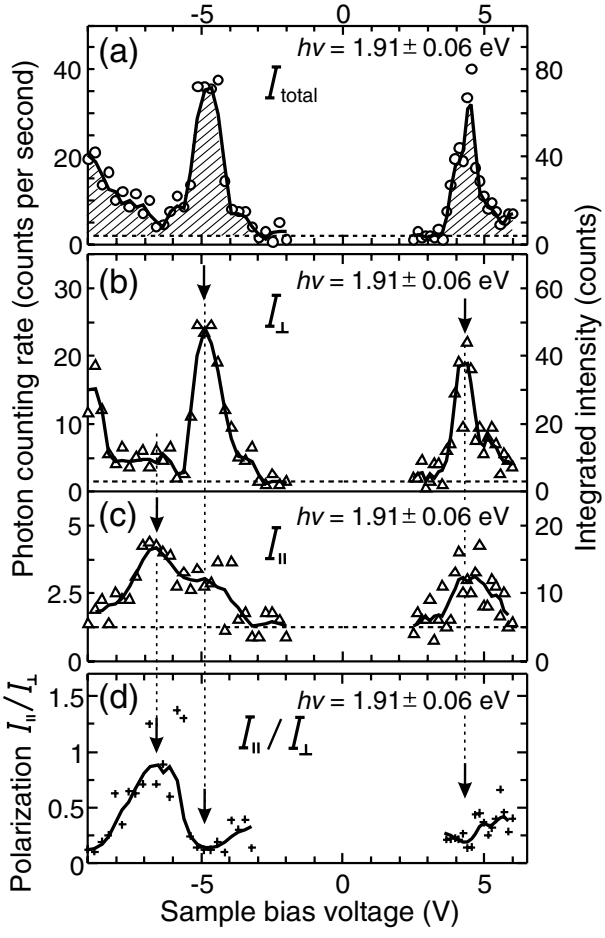

FIG. 3. (a) Total intensity I_{total}, (b) p-polarized intensity $I_\perp$, and (c) s-polarized intensity $I_\parallel$ of the emitted light from the gap between a STM tip and a Si(001)-(2×1) sample as a function of V_s at $I_t = 8$ nA and $h\nu = 1.91$ eV (± 0.06 eV). (d) The ratio $I_\parallel / I_\perp$ as a function of V_s. In the figures, solid curves show fittings to the data, and horizontal broken lines show the dark count level.

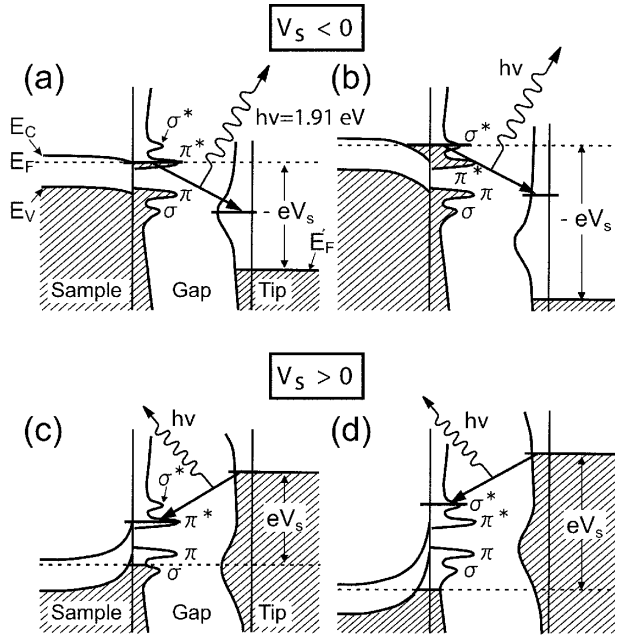

FIG. 4. (a)–(d) Schematic diagram of the light creation process with an energy of 1.91 eV in the tip-sample gap formed by a n-type Si(001) sample and a metal tip under four different V_s conditions. In the energy diagram, E_c is the bottom of the conduction band, E_v is the top of the valence band, E_F is the Fermi level of the sample, and E_F' is the Fermi level of the tip.

occupied state near the Fermi level of the tip to the π^* state of the sample as shown in Fig. 4(c). The transition illustrated in Fig. 4(d) is not observed in Fig. 3(a) because it should occur out of the experimental range of V_s in Fig. 3(a).

Figures 3(b) and 3(c) show the intensities of the p- and s-polarized components of the emitted light $I_\perp$ and $I_\parallel$, respectively, measured at the same photon energy $h\nu =$ 1.91 eV ($\pm$ 0.06 eV). The measurements of $I_\perp$ and $I_\parallel$ were made using the right optical fiber bunch, whereas I_{total} mentioned above was measured using the left optical fiber bunch. As we can see, $I_\perp$ and $I_\parallel$ exhibit different V_s dependences. Namely, $I_\perp$ shows its maximum at $V_s = -4.8$ eV [Fig. 3(b)], but the maximum of $I_\parallel$ is seen at $V_s = -6.5$ eV [Fig. 3(c)]. As a result, the ratio $I_\parallel/I_\perp$ plotted in Fig. 3(d) shows a strong maximum at $V_s = -6.5$ eV, indicating an important fact discussed below.

The polarized light emission from the tip-sample gap of the STM described above is interpreted as follows. The light creation process is described by the quantum field theory, where photons are spontaneously created by the interaction between atomic electrons and the radiation field [14], and the matrix element of the interaction H_{int} is expressed as

$$\langle B|H_{\text{int}}|A\rangle = e\sqrt{\frac{\hbar\omega}{2\epsilon_0 V}}\langle B|\mathbf{r}|A\rangle \cdot \hat{\mathbf{e}}_a e^{i\omega t}, \qquad (1)$$

where $|A\rangle$ is the initial occupied state, $|B\rangle$ is the final empty state, $\hat{\mathbf{e}}_a$ is a unit vector representing the polarization direction of the light, ϵ_0 is the free space permittivity, V is the volume of the system, and $\mathbf{r}$ is a position vector. The energy of photons created corresponds to the energy difference between the initial and final states: $\hbar\omega = E_A - E_B$. In the case of the light emission from the tip-sample gap of the STM, the narrow gap allows an electron to make direct transition across the gap [8]. As is noted from Eq. (1), the direction of an electric dipole induced by the transition is determined by the matrix element vector $\langle B|\mathbf{r}|A\rangle$.

We consider radiation due to the electric dipole induced by the direct electronic transition in the narrow gap of the STM. The geometry of the gap modifies the induced electric dipole as $\mathbf{P}(\omega) = \boldsymbol{\alpha}(\omega) \cdot \langle B|e\mathbf{r}|A\rangle$, where $\boldsymbol{\alpha}(\omega)$ is a matrix determined by the shapes and dielectric functions of the tip and sample [15]. The electric field radiated from this dipole $\mathbf{P}(\omega)$ is detected at a far field distance. The field is calculated by solving the Helmholz equation using a technique similar to that applied in the calculations of the radiation from an antenna on the earth's surface [16]. When the electric dipole is placed at the origin with the orientation along the z axis perpendicular to the sample surface, the electric field at a far field distance is expressed in spherical coordinates as

$$\mathbf{E}_{\text{far},\perp}(r,\theta) = k^2 \frac{P_z(\omega)}{4\pi\epsilon_0}\frac{e^{ikr-i\omega t}}{r}\sin\theta(1 + V_{zz}(\theta))\hat{\mathbf{e}}_\theta. \quad (2)$$

When the dipole is placed at the origin with the orientation along the x axis parallel to the sample surface, the electric field is expressed as

$$\mathbf{E}_{\text{far},\parallel}(r,\theta,\phi) = k^2 \frac{P_x(\omega)}{4\pi\epsilon_0}\frac{e^{ikr-i\omega t}}{r}\{[\cos\theta\cos\phi(1 + V_{xx}(\theta)) - \sin\theta V_{xz}(\theta)]\hat{\mathbf{e}}_\theta + \sin\phi(1 + V_{xx}(\theta))\hat{\mathbf{e}}_\phi\}, \qquad (3)$$

where k is the wave vector, $V_{zz}(\theta)$, $V_{xx}(\theta)$, and $V_{xz}(\theta)$ are the Fresnel reflection coefficients determined by boundary conditions, and $\hat{\mathbf{e}}_\theta$ and $\hat{\mathbf{e}}_\phi$ are unit vectors in spherical coordinates. With the notation used in Eqs. (2) and (3), $V_{ij}(\theta)$ means the reflection coefficient of the i component ($i = x, z$) of the incident wave to the j component ($j = x, z$) of the reflected wave. If the parameters $V_{xx}(\theta)$, $V_{zz}(\theta)$, and $V_{xz}(\theta)$ are zero, Eqs. (2) and (3) yield electric fields radiated from a single electric dipole in free space.

Calculations of Eqs. (2) and (3) using the bulk dielectric functions of the materials of our tip (W) and sample (Si) provide the following features. First, the radiation process from the electric dipole on a Si surface is energy independent in the visible spectral range. This indicates that the observed V_s-dependent features are due to the light creation process. Second, since the geometric arrangement of the tip and the sample has an axial symmetry approximately, the matrix $\alpha(\omega)$ is diagonal [17]. Then Eqs. (2) and (3) yield a simple relationship between the

electric dipole induced by the radiative transition and polarization of the light at a far field distance. For example, in the transition from the p_z orbital of the sample to the d_{z^2} orbital of the tip [18,19], the axial symmetry of each wave function in the matrix element vector provides a nonzero z component $\langle d_{z^2}|z|p_z\rangle$. Therefore, as expressed in Eq. (2), the dipole transition creates p-polarized light. The situation is schematically illustrated in Fig. 2(d). Similarly, the dipole transition from the p_x orbital of the sample to the d_{z^2} orbital of the tip creates s-polarized light as illustrated in Fig. 2(e). Finally, calculation of the intensity of radiation from a dipole on a Si surface indicates that $|\mathbf{E}_{\mathrm{far},\perp}|^2$ is 6 times larger than $|\mathbf{E}_{\mathrm{far},\parallel}|^2$ [20]. This difference explains the experimental result that the averaged intensity of $I_\parallel$ [Fig. 3(c)] is much smaller than that of $I_\perp$ [Fig. 3(b)].

The polarization of the isochromat light at three different V_s marked by the vertical dashed lines in Fig. 3 is interpreted by the above-mentioned mechanism. The peak at $V_s = -4.8$ V in Fig. 3(b) is due to a radiative transition from the π^* state of the sample to an empty state of the tip as shown in Fig. 4(a). Since the π^* state of a buckled Si dimer is mainly formed by the $2p_z$ orbital [11,12] [see Fig. 2(b)] and since the tip with a W surface has an electronic state formed by the $6d_{z^2}$ orbital at energies of 1–2 eV above E_F [21,22], the radiative dipole transition expressed by $\langle d_{z^2}|\mathbf{r}|p_z\rangle$ induces an electric dipole directed along the z axis. In Eq. (2), radiation from the electric dipole P_z causes p-polarized light. This agrees with the experimental result that $I_\perp$ in Fig. 3(b) has its maximum at $V_s = -4.8$ V. The peak at $V_s = -6.5$ V in Fig. 3(c) is due to a radiative transition from the σ^* state of the sample to an empty surface state of the tip as shown in Fig. 4(b). The σ^* state is mainly formed by $2p_x$ orbitals [see Fig. 2(b)], and the radiative transition from the $2p_x$ orbitals to the $6d_{z^2}$ orbital creates an electric dipole directed along the x axis, which causes s-polarized light emission. This is the reason why $I_\parallel$ in Fig. 3(c) exhibits its maximum at $V_s = -6.5$ eV. Calculation of radiation from the dipole P_x using Eq. (3) leads to the same order of p ($\hat{\mathbf{e}}_\theta$ component) and s ($\hat{\mathbf{e}}_\phi$ component) polarized light intensity and yields a ratio $(I_\parallel/I_\perp)$ of ~ 1. This is consistent with the experimental result at $V_s = -6.5$ V [see Fig. 3(d)]. At $V_s = +4.2$ V, the radiative transition from the $6d_{z^2}$ orbital of the tip with an energy near the Fermi level [18,19] to the empty π^* state of the sample [see Fig. 4(c)] causes an electric dipole P_z, which produces p-polarized light. Therefore, $I_\perp$ in Fig. 3(b) has its maximum at $V_s = +4.2$ V. These agreements of the experimental results [Figs. 3(a)–3(d)] with the dipole transition theory [Eqs. (1)–(3)] mean that the optical selection rules hold in the light emission of concern.

In conclusion, it has been revealed that light emission from the tunneling gap between the STM tip made of W and the Si sample with a (001)-(2×1) surface is fully described by the dipole transition theory. Namely, optical selection rules still apply in the light emission. This not only indicates that direct electronic transitions between the tip and the sample occur, but also suggests that orbital symmetries of surface states can be analyzed in an energy-resolved manner at the spatial resolution of STM.

[1] J. K. Gimzewski, B. Reil, J. H. Coombs, and R. R. Schlittler, Z. Phys. B **72**, 497 (1988).

[2] R. Berndt, J. K. Gimzewski, and P. Johansson, Phys. Rev. Lett. **67**, 3796 (1991).

[3] P. Johansson, R. Monreal, and P. Apell, Phys. Rev. B **42**, 9210 (1990).

[4] B. N. J. Persson and A. Baratoff, Phys. Rev. Lett. **68**, 3224 (1992).

[5] D. L. Abraham, A.Veider, Ch. Schönenberger, H. P. Meier, D. J. Arent, and S. F. Alvarado, Appl. Phys. Lett. **56**, 1564 (1990).

[6] L. Samuelson, J. Lindahl, L. Montelius, and M.-E. Pistol, Phys. Scr. **T42**, 149 (1992).

[7] A. Downes and M. Welland, Phys. Rev. Lett. **81**, 1857 (1998).

[8] C. Thirstrup, M. Sakurai, K. Stokbro, and M. Aono, Phys. Rev. Lett. **82**, 1241 (1999).

[9] The transmission ratio of the two orthogonal polarization components through a Polarcor polarizer is 1:10 000 in the range of 630–700 nm. An optical band-pass filter positioned in front of the detector was selected to allow light transmission with an energy of 1.91 ± 0.06 eV, which is within the wavelength range of the polarizer.

[10] F. J. Himpsel, Adv. Phys. **32**, 1 (1983).

[11] P. Kruger, A. Mazur, J. Pollmann, and G. Wolfgarten, Phys. Rev. Lett. **57**, 1468 (1986).

[12] A. Ramstad, G. Brocks, and P. J. Kelley, Phys. Rev. B **51**, 14504 (1995).

[13] M. McEllistrem, G. Haase, D. Chen, and R. J. Hamers, Phys. Rev. Lett. **70**, 2471 (1993).

[14] J. J. Sakurai, *Advanced Quantum Mechanics* (Addison-Wesley, New York, 1967).

[15] E. Anisimovas and P. Johansson, Phys. Rev. B **59**, 5126 (1999).

[16] A. Sommerfeld, *Partial Differential Equations of Physics* (Academic, New York, 1949).

[17] An asymmetrical configuration of the tip-sample geometry induces the mixing of each polarized light. Since the mixed light intensity depends weakly on energy of the light in the present system, the mixed component does not explain the energy dependent spectra. The contribution can be neglected.

[18] C. J. Chen, *Introduction to Scanning Tunneling Microscopy* (Oxford University Press, Oxford, 1993).

[19] S. Ohnishi and M. Tsukada, Solid State Commun. **71**, 391 (1989).

[20] In the case of metal sample surfaces, the difference becomes much larger. Then only p-polarized light is observed experimentally.

[21] L. F. Mattheiss and D. R. Hamann, Phys. Rev. B **29**, 5372 (1984).

[22] I. R. Collins, A. D. Laine, and P.T. Andrews, J. Phys. Condens. Matter **4**, 2891 (1992).